Jurnal Rekayasa Mesin
p-ISSN: 1411-6863, e-ISSN: 2540-7678
Vol.21, No.1, April **2025**, p. 31-38

Limitations of Interlocking Features in Rotary Friction Welding (RFW) of 3D-printed PLA

Fauzan Al Fathurrahman, Fathur Rahman Naufal Santoso, Erwin, Didik Sugiyanto, Juan Pratama*
Departement of Mechanical Engineering, Faculty of Engineering, Universitas Darma Persada
Jl. Taman Malaka Selatan No. 8, RW. 6, Pondok Kelapa, Duren Sawit, Jakarta Timur, DKI Jakarta. 13450
*E-mail: juan_pratama@ft.unsada.ac.id/juanprtm@gmail.com

Submitted: 29-01-2026; Accepted: 25-04-2026; Published: 30-04-2026

Abstract

The limited build volume of fused deposition modeling (FDM) often necessitates the use of joining methods for larger components. However, the effectiveness of interlocking features in the RFW of 3D-printed polymers remains unclear. This study investigates the limitations of interlocking features in RFW of polylactic acid (PLA) by evaluating the effect of male-female geometry on the joint performance. The results show that all interlocked RFW joints exhibit significantly reduced tensile strength, reaching only approximately 30% of the control samples, accompanied by decreased ductility. Despite variations in the interlock geometry, no significant improvement in joint performance was observed. Failure analysis indicates that the excessive weld flash accumulation within the interlocking region generates internal pressure, which restricts material flow and promotes crack initiation. This leads to localized plastic deformation followed by brittle failure at the joint interface. These findings demonstrate that the interlocking geometry does not necessarily enhance joint quality in RFW of 3D-printed PLA and may introduce inherent limitations if not properly designed. This study highlights the critical role of material flow and geometric constraints in governing joint performance, emphasizing the need for optimized interlock design and process control in thermoplastic friction welding.

Keywords: FDM; interlocking; joint performance; PLA; RFW

Abstrak

Keterbatasan volume pencetakan pada proses *fused deposition modeling* (FDM) sering kali memerlukan penggunaan metode penyambungan untuk menghasilkan komponen berukuran lebih besar; namun, efektivitas geometri *interlocking* dalam *rotary friction welding* (RFW) pada material polimer hasil pencetakan 3D masih belum dipahami secara jelas. Penelitian ini bertujuan untuk mengkaji keterbatasan fitur *interlocking* pada proses RFW material *polylactic acid* (PLA) dengan mengevaluasi pengaruh geometri sambungan *male–female* terhadap kinerja sambungan. Hasil penelitian menunjukkan bahwa seluruh sambungan RFW dengan *interlocking* mengalami penurunan kekuatan tarik yang signifikan, yaitu hanya mencapai sekitar 30% dibandingkan dengan sampel kontrol, serta diikuti dengan penurunan keuletan. Meskipun dilakukan variasi geometri *interlocking*, tidak ditemukan peningkatan performa sambungan yang signifikan. Analisis kegagalan menunjukkan bahwa akumulasi *weld flash* yang berlebihan pada daerah *interlocking* menghasilkan tekanan internal yang membatasi aliran material dan memicu inisiasi retak. Kondisi ini menyebabkan terjadinya deformasi plastis lokal yang diikuti oleh kegagalan getas pada area sambungan. Temuan ini menunjukkan bahwa penggunaan geometri *interlocking* tidak selalu meningkatkan kualitas sambungan pada proses RFW material PLA hasil pencetakan 3D, dan bahkan dapat menimbulkan keterbatasan jika tidak dirancang secara tepat. Penelitian ini menekankan pentingnya peran aliran material dan batasan geometris dalam menentukan kinerja sambungan, serta perlunya optimasi desain *interlock* dan pengendalian proses dalam pengelasan gesek material termoplastik.

Kata kunci: FDM; performa sambungan; PLA; penguncian; RFW

1. Introduction

Through its layer-by-layer processing method, additive manufacturing enables the fabrication of complex parts with tailored material and mechanical properties [1]. Fused Filament Fabrication (FFF), also referred to as Fused Deposition Modeling (FDM), become the most prevalent additive manufacturing technique due to its use of abundant availability of polymer filaments [2]. Polylactic acid (PLA), on the other hand, become one of the most extensively used polymer filaments in FDM due to its biodegradable nature, favorable mechanical properties, and ease of processing [3]. Rapid advancements in this technique, combined with PLA as the base material, have enabled its adoption in various applications, spanning from the automotive industry to biomedical engineering [4-9]. Despite its advantages, this technique is often constrained by the build volume of the machine, which is typically limited in size [10]. To address this limitation, FDM products could be segmented into multiple parts and subsequently assembled using mechanical joining, such as nuts and clamping [11,12]. However, this method may result in the formation of microcracks at the joint interfaces, potentially compromising structural integrity [13]. Consequently, there is a need for alternative joining techniques, especially for Fused Deposition Modeled parts.

Solid-state joining, such as rotary friction welding (RFW), is recognized as a more sustainable and environmentally friendly joining technique due to its reduced energy consumption and limited environmental impact [14]. Traditionally, this method has been applied mainly to metals, benefiting from its versatility in joining dissimilar materials across a broad range of applications [15-17]. In recent years, RFW has increasingly been applied to polymer joining, as the relatively low joining temperatures required for polymers can be readily achieved through this process. Earlier research indicates that RFW is capable of joining 3D-printed PLA and ABS, although the fatigue performance remains inferior to that of homogeneous PLA/PLA or ABS/ABS joints [18]. Additional research has reported successful joining between 3D-printed PLA and PLA-metal composite, indicated by enhanced bending strength and surface hardness relative to the base material [19]. In the RFW process, rotational speed is a critical parameter that significantly influences joint strength as the rotational speed increases [13]. On the other hand, incorporating an ultrasonic vibration into the RFW process has been shown to enhance the joint performance of 3D-printed PLA [20]. In addition to process parameters, RFW joint performance can be enhanced by tailoring the joint profile shape, such as dividing the interface into interlocking male and female sections [21]. By applying this approach, the weld flash generated during the joining process is trapped within the female profile and mechanically locked when cooled, which is expected to enhance joint quality in the interfacial region. Moreover, RFW enables localized heating and material flow at the interface, which is essential for evaluating the effectiveness of the interlocking geometry in enhancing mechanical bonding [22]. Nevertheless, the application of this method to polymer RFW, specifically for 3D-printed parts, has not been reported in the literature, highlighting a gap for this research. Eventually, this study aims to evaluate the effect of interlocking on the RFW process by investigating the influence of male-female joint profile geometry on the joint quality of 3D-printed PLA.

2. Material and Method

The tensile strength of the welded specimens was used as the criterion to evaluate the joint quality of PLA/PLA samples. The samples were manufactured from PLA+ filament (eSun Filament, China) using a Bambu Lab A1 3D printer, and the corresponding printing parameters are presented in Table 1.

Table 1. Printing parameters for samples fabrication

Parameters	Value
Layer height	0.2 mm
Printing Temperature	210 °C
Printing Speed	35 mm/mins
Printing Orientation	Vertical build
Raster Angle	45°/-45°
Infill Density	100%

Cylindrical samples were prepared following the ASTM E8 standard, incorporating male feature diameters of 1, 3, and 5 mm. As shown in Figure 1, the male feature length was maintained at 1,5 mm, and selected to ensure mechanical engagement between male-female features, as shorter features may result in inadequate interlocking, while longer features could cause material accumulation. In addition, control samples were also produced using identical printing parameters to serve as tensile strength references, without being subjected to the RFW process. The design of experiment (DoE) is summarized in Table 2, with five samples prepared for each group, resulting in a total of 20 samples.

Table 2. Design of Experiment of this research

Run	Group Code	Male diameter	Method	Number of Samples
1	Control	-	Fully printed	5
2	A	1 mm	RFW at 2000 rpm	5
3	B	3 mm	RFW at 2000 rpm	5
4	C	5 mm	RFW at 2000 rpm	5
		Total Samples		20

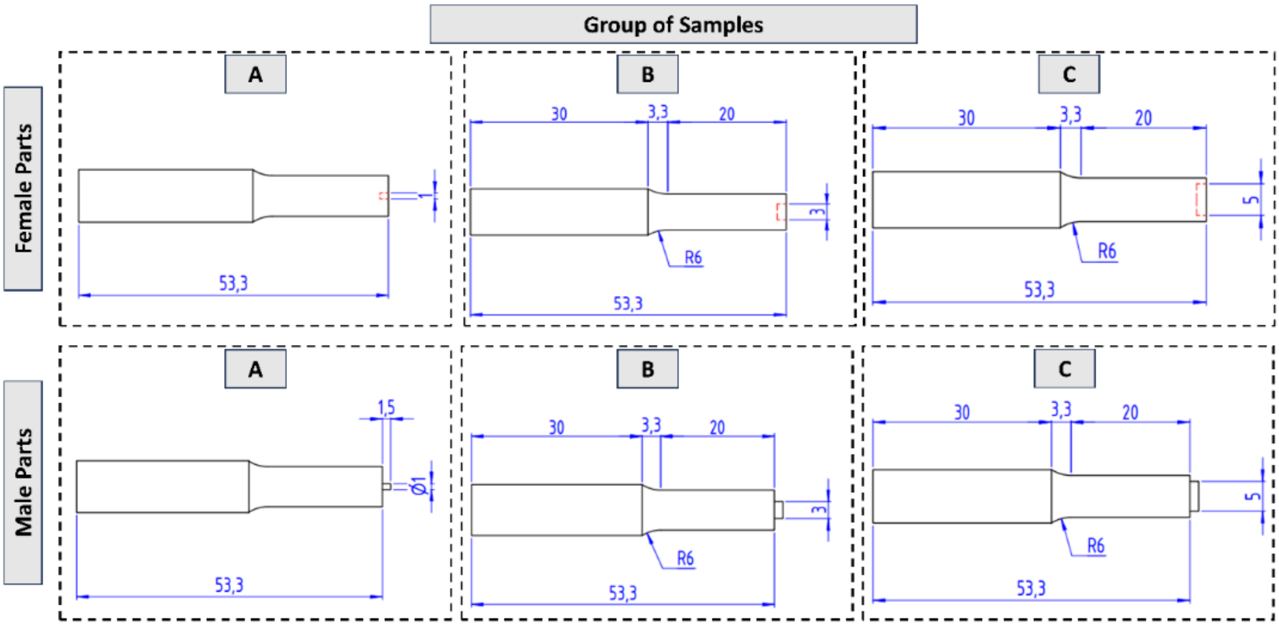

Figure 1. Design and dimensions of RFW specimens for each experimental group

The RFW process was performed on a Magnum-Tech FEL-1640 lathe, with the spindle speed maintained at 2000 rpm across all male-female feature configurations. The rotational speed was selected based on prior studies on rotary friction welding of thermoplastic materials, which suggest that an adequate level of rotational speed is necessary to generate sufficient frictional heat while preventing thermal degradation [22]. During the joining process, the male feature was rotated, while the female feature remained stationary and advanced toward the male feature at a constant speed of 2 mm/min via the tailstock, as shown in Figure 2. The process was conducted until a penetration depth of 1,5 mm was reached, using friction, forging, and cooling times of 15 s, 10 s, and 10 s, respectively. Once the RFW process was completed, excess weld flash on the joined samples was removed by lathe machining. After sample preparation, tensile tests were conducted using a Tensilon RTF-2410 universal testing machine following the ASTM E8 standard, at a constant crosshead speed of 10 mm/min for all the variations of group samples. After tensile testing, the fracture mode was examined through macrostructural observation on the fracture area using Dinolite AF3113T optical microscope at a magnification of 20×.

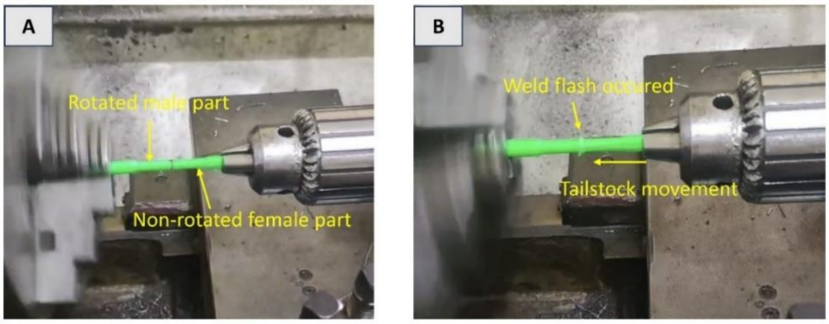

Figure 2. RFW process using a lathe: (A) initiation of the process, and (B) tailstock movement during welding

3. Results and Discussion

The tensile test results for each sample group are presented in Figure 3. From the figure, it can be seen that the control sample exhibits an ultimate tensile strength (UTS) of 21.88 ± 0.3 MPa, a strain at break of 3.42 ± 0.93 %, and an elastic modulus of 1162.88 ± 389.8 MPa. These results are in close agreement with those reported in previous studies [23], thereby validating the findings of the present test.

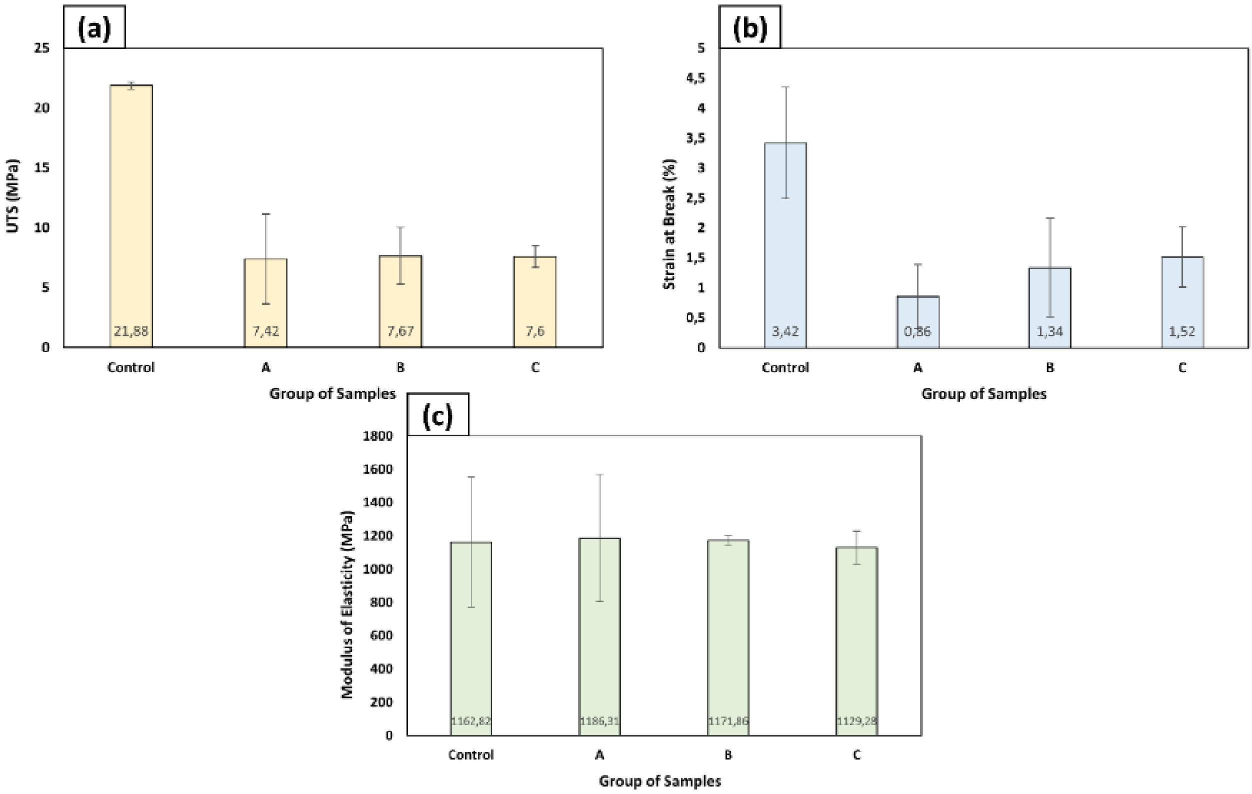

Figure 3. Graphical representation of tensile properties for each sample group: (a) UTS, (b) strain at break, and (c) elastic modulus

As shown in Figure 3 (a), the UTS of groups A, B, and C exhibits a substantial reduction compared to the control group, with all samples subjected to the RFW process using male-female interlocking achieving only approximately 30% of the control UTS. This result deviates from several previous studies, where RFW of homogeneous materials was reported to produce joints with favorable performance [13,19,24]. Notably, the present study differs from earlier research by introducing variations in male-female interlocking features within the RFW process. Despite expectations, the present results show a substantial decline in tensile strength, implying that RFW joints with male-female interlocking fail to achieve adequate joint performance. Furthermore, the ANOVA results presented in Table 3 indicate that there is no statistically significant difference among the UTS of the RFW sample groups (p-value > 0,05), suggesting that the variation in interlocking geometry does not lead to a significant improvement in joint performance.

In addition to the reduction in UTS, a decrease in strain at break is also observed, as shown in Figure 3 (b), indicating embrittlement of the RFW samples. However, a different trend is observed, with a slight increase in strain as the male feature dimensions increase, although the change is not statistically significant based on the deviation. On the other hand, no significant differences in elastic modulus are observed between the control and RFW samples, as shown in Figure 3 (c), which also contrasts with previous studies.

Table 3. One-way ANOVA test on the UTS value and comparison of each group

Difference of Levels	Difference of Means	SE of Difference	95% CI	T-Value	Adjusted P-Value
A Vs Control	-14,46	1,43	(-17,50; -11,42)	-10,08	0,000
B Vs Control	-14,21	1,43	(-17,25; -11,17)	-9,91	0,000
C Vs Control	-14,28	1,43	(-17,32; -11,24)	-9,96	0,000
B Vs A	0,25	1,43	(-2,79; 3,29)	0,18	0,863
C Vs A	0,18	1,43	(-2,86; 3,22)	0,13	0,899
C Vs B	-0,07	1,43	(-3,11; 2,97)	-0,05	0,963

Simultaneous confidence level = 81,11%

3.1. Failure Analysis

During the RFW process, the axial penetration resulting from contact between the two materials generates a weld flash around the joint due to the localized temperature increase. Within the male-female features, the weld flash formed during RFW was expected to be retained internally, contributing to mechanical interlocking and potentially improving joint integrity. The weld flash generally presents a refined structure caused by mechanical deformation, leading to localized hardening and the development of a heat-affected zone (HAZ) in the adjacent region [25]. As shown in Figure 4, excessive filling of the male-female features by the weld flash resulted in the development of internal pressure within the joint. The resulting internal pressure may induce stress concentration at the interlock interface, facilitating microcrack initiation and leading to premature joint failure [26,27], which contributes to the reduced tensile strength observed in the RFW samples. In addition, interlocking may restrict the viscous flow of softened PLA, leading to incomplete molecular diffusion across the interface. During the joint formation process, the concentration of weld flash and the HAZ within the female feature promotes localized bonding and tensile loading on this region, leading to crater-hill formation upon failure, which indicates embrittlement in this area. This phenomenon is evident from the macrostructural observations shown in Figure 5, where the crater-hill features are observed in all RFW samples. This behavior is indicative of localized plastic deformation at the joint interface, followed by brittle failure, likely due to stress concentration and restricted material flow within the interlocking region. In addition, the build orientation during printing may also contribute to joint failure at the interlock region. This is primarily attributed to the vertical build orientation, in which interlayer interfaces are aligned perpendicular to the applied tensile load, resulting in weaker interlayer bonding and increased susceptibility to failure [28], especially at the interlock region. This weak interlayer bonding reflects inefficient stress transfer between layers [23], which can promote crack initiation under internal pressure generated by the weld flash, as evidenced by the macrostructural observation shown in Figure 5.

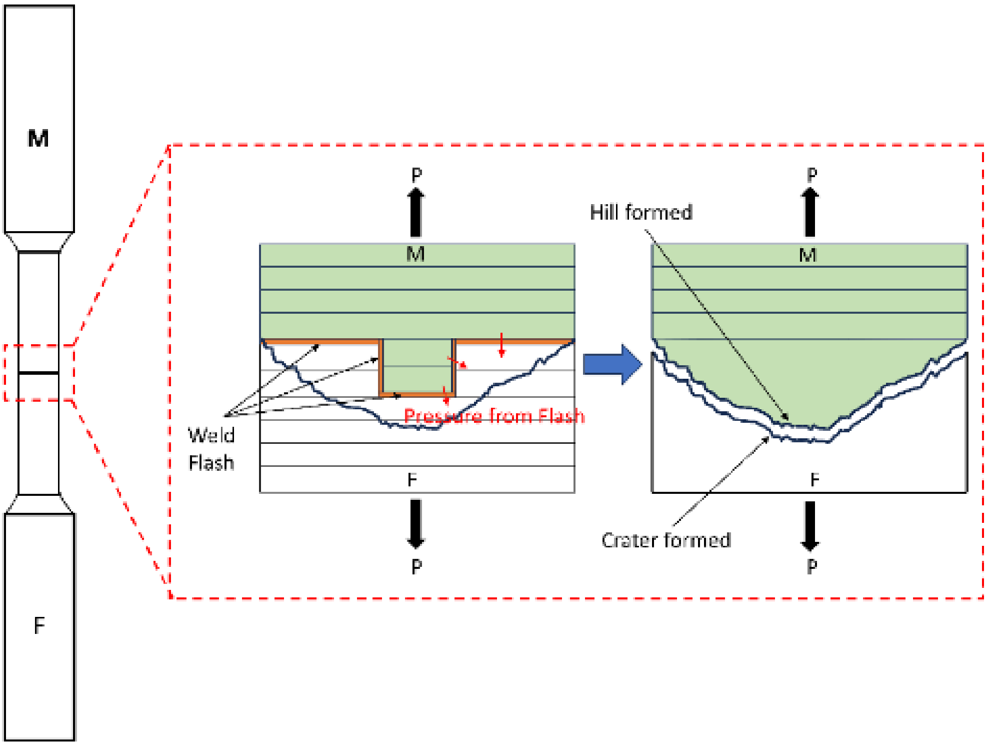

Figure 4. Schematic illustration of internal pressure formation caused by weld flash accumulation and the resulting crater-hill morphology

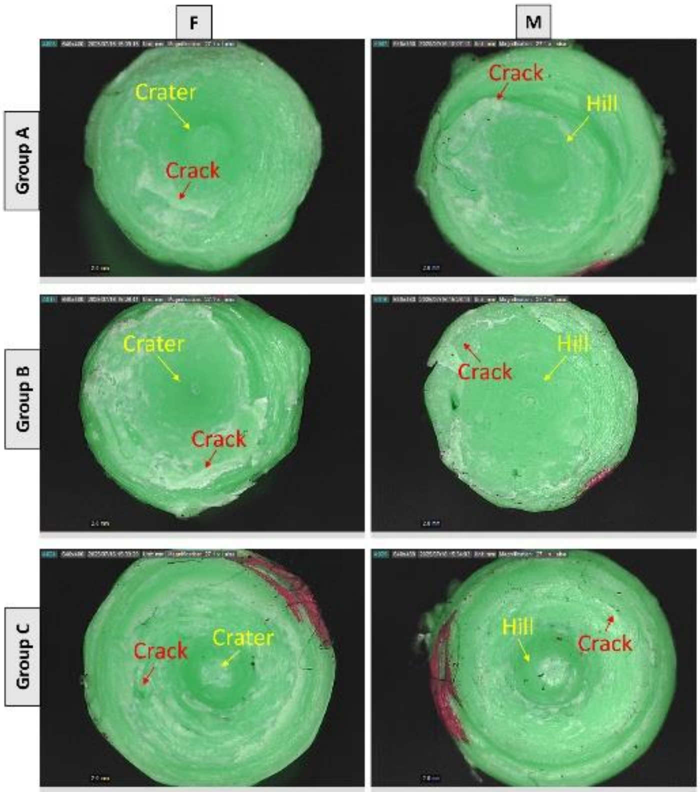

Figure 5. Results of macrostructural observations of the RFW-joined samples

4. Conclusion

This study demonstrates that the application of interlocking features in RFW of 3D-printed PLA does not necessarily enhance joint performance, but instead introduces critical limitations. Despite the intended mechanical interlocking effect, all RFW samples exhibited significantly reduced tensile strength, reaching only approximately 30% of the control, accompanied by reduced ductility. The findings reveal that the presence of interlocking features promotes localized material accumulation in the form of weld flash, which generates internal pressure within the joint region. This condition leads to localized plastic deformation followed by brittle failure, ultimately governing the joint performance. These results indicate that the failure is not merely due to insufficient bonding, but is strongly influenced by geometric constraints that restrict material flow and induce stress concentration.

This study provides a key insight that interlocking features, when applied to thermoplastic rotary friction welding, may be inherently limited if not properly designed. Therefore, the design of the interlocking features must carefully consider dimensional tolerance, material flow behavior, and build orientation to avoid detrimental internal pressure effects. The implications of this work highlight that optimization of joint geometry is as critical as process parameters in achieving reliable RFW joints. Future work should focus on redesigning interlock configurations, controlling weld flash distribution, and integrating the process-structure relationship properly to overcome the identified limitations and improve joint performance. Eventually, this finding is particularly relevant for the design of advanced joining strategies in additive manufacturing applications.

Acknowledgement

This research was funded by Hibah Internal Universitas Darma Persada 2025/2026.

References

[1] A. Y. Anggara, G. A. Saputra, D. Sugiyanto, and J. Pratama, “Evaluation of a Nylon 3D-Printed Wrist Splint Through Finite Element Analysis (FEA) and User-Based Assessment,” *J. Rekayasa Mesin*, vol. 20, no. 3, pp. 513–520, 2025.

[2] U. Agus Salim *et al.*, “Microhole Creation in FDM-Printed Sheet Polymers: A Punching Process Approach,” *Indones. J. Comput. Eng. Des.*, vol. 6, no. 2, pp. 108–118, Oct. 2024, doi: 10.35806/8r45gs31.

[3] Z. Oksiuta, M. Jalbrzykowski, J. Mystkowska, E. Romanczuk, and T. Osiecki, “Mechanical and Thermal Properties of Polylactide (PLA) Composites Modified with Mg, Fe, and Polyethylene (PE) Additives,” *Polymers (Basel).*, vol. 12, no. 12, p. 2939, Dec. 2020, doi: 10.3390/polym12122939.

[4] A. Z. Adib *et al.*, “Flexural strength of the sandwich-structured parts made of polylactic-acid and thermoplastic-polyurethane fabricated by using extrusion-based multi-material additive manufacturing,” *Int. J. Adv. Manuf. Technol.*, vol. 132, no. 9–10, pp. 4805–4827, Jun. 2024, doi: 10.1007/s00170-024-13608-6.

[5] A. Andrearczyk, B. Konieczny, and J. Sokołowski, “Additively Manufactured Parts Made of a Polymer Material Used for the Experimental Verification of a Component of a High-Speed Machine with an Optimised Geometry—Preliminary Research,” *Polymers (Basel).*, vol. 13, no. 1, p. 137, Dec. 2020, doi: 10.3390/polym13010137.

[6] J. P. Budi Arifvianto, Muslim Mahardika, *Manufaktur Aditif Material Polimer*. UGM PRESS, 2022. doi: https://books.google.co.id/books?hl=en&lr=&id=eoNoEQAAQBAJ&oi=fnd&pg=PA31&dq=info:FMBfxhipFcwJ:scholar.google.com&ots=0yQ1GZrmHt&sig=qle4nVCG88EmGbWF1fBIW2iV83s&redir_esc=y#v=onepage&q&f=false.

[7] S. Farah, D. G. Anderson, and R. Langer, “Physical and mechanical properties of PLA, and their functions in widespread applications — A comprehensive review,” *Adv. Drug Deliv. Rev.*, vol. 107, pp. 367–392, Dec. 2016, doi: 10.1016/j.addr.2016.06.012.

[8] J. Pratama *et al.*, “A Review on Reinforcement Methods for Polymeric Materials Processed Using Fused Filament Fabrication (FFF),” *Polymers (Basel).*, vol. 13, no. 22, p. 4022, Nov. 2021, doi: 10.3390/polym13224022.

[9] L. Sandanamsamy *et al.*, “A comprehensive review on fused deposition modelling of polylactic acid,” *Prog. Addit. Manuf.*, vol. 8, no. 5, pp. 775–799, Oct. 2023, doi: 10.1007/s40964-022-00356-w.

[10] A. Bagheri, M. S. Aghareb Parast, A. Kami, M. Azadi, and V. Asghari, “Fatigue testing on rotary friction-welded joints between solid ABS and 3D-printed PLA and ABS,” *Eur. J. Mech. - A/Solids*, vol. 96, no. January, p. 104713, Nov. 2022, doi: 10.1016/j.euromechsol.2022.104713.

[11] H. Wu, J. Li, H. Liu, and D. Zuo, “Time - varying thermoelastic coupling analysis of heat source of ball screw feed

drive system," *Int. J. Adv. Manuf. Technol.*, pp. 923–939, 2023, doi: 10.1007/s00170-023-12352-7.

[12] N. A. Panc, V. Bocaneț, C. Vilău, H. Chezan, I. A. Popan, and G. Conțiu, "New method of fixturing the low-rigidity parts by adhesive clamping," *Int. J. Adv. Manuf. Technol.*, vol. 129, no. 5–6, pp. 2591–2608, Nov. 2023, doi: 10.1007/s00170-023-12429-3.

[13] C. C. Kuo, H. X. Liang, S. H. Huang, and S. F. Tseng, "Enhancing the Weld Quality of Polylactic Acid Biomedical Materials Using Rotary Friction Welding," *Polymers (Basel).*, vol. 16, no. 7, 2024, doi: 10.3390/polym16070991.

[14] N. Vidakis, M. Petousis, A. Korlos, N. Mountakis, and J. D. Kechagias, "Friction Stir Welding Optimization of 3D-Printed Acrylonitrile Butadiene Styrene in Hybrid Additive Manufacturing," *Polymers (Basel).*, vol. 14, no. 12, p. 2474, Jun. 2022, doi: 10.3390/polym14122474.

[15] Y. Wang *et al.*, "Interfacial microstructure and mechanical properties of rotary inertia friction welded dissimilar 422 martensitic stainless steel to 4140 low alloy steel joints," *Mater. Sci. Eng. A*, vol. 885, no. April, p. 145607, Oct. 2023, doi: 10.1016/j.msea.2023.145607.

[16] M. Farbakhti, S. R. Elmi Hosseini, S. A. Mousavi Mohammadi, S. Sadatabhari, H. Yuan-ming, and R. Li, "Similar and dissimilar rotary friction welding of steels: A review of microstructural evolution and mechanical properties," *J. Mater. Res. Technol.*, vol. 36, no. May, pp. 8777–8803, May 2025, doi: 10.1016/j.jmrt.2025.05.079.

[17] S. Delijaicov *et al.*, "Microhardness and residual stress of dissimilar and thick aluminum plates AA7181-T7651 and AA7475-T7351 using bobbin, top, bottom, and double-sided FSW methods," *Int. J. Adv. Manuf. Technol.*, vol. 108, no. 1–2, pp. 277–287, May 2020, doi: 10.1007/s00170-020-05370-2.

[18] M. S. A. Parast, A. Bagheri, A. Kami, M. Azadi, and V. Asghari, "Bending fatigue behavior of fused filament fabrication 3D-printed ABS and PLA joints with rotary friction welding," *Prog. Addit. Manuf.*, vol. 7, no. 6, pp. 1345–1361, Dec. 2022, doi: 10.1007/s40964-022-00307-5.

[19] C.-C. Kuo, H.-W. Chen, and S.-H. Huang, "Rotary Friction Welding of Dissimilar Polymer Rods Containing Metal Powder," *Polymers (Basel).*, vol. 15, no. 22, p. 4354, Nov. 2023, doi: 10.3390/polym15224354.

[20] C.-C. Kuo, H.-W. Chen, A. Farooqui, S.-H. Huang, and S.-F. Tseng, "Enhancing the mechanical integrity of Polylactic acid components via ultrasound-assisted rotary friction welding for sustainable medical device fabrication," *J. Manuf. Process.*, vol. 141, pp. 1324–1336, May 2025, doi: 10.1016/j.jmapro.2025.03.052.

[21] Y. Purwaningrum, F. Fatha, and A. Data Pratama, "Optimasi Sambungan Rotary Friction Welding (Rfw) Pada Aluminium 4017 Dengan Variasi Bentuk Profil Sambungan," *Simp. Nas. RAPI XXI-2022 FT UMS*, no. 2022: Prosiding Simposium Nasional Rekayasa Aplikasi Perancangan dan Industri, pp. 165–170, 2022, [Online]. Available: https://proceedings.ums.ac.id/rapi/article/view/2616

[22] C.-C. Kuo, N. Gurumurthy, H.-W. Chen, and S.-H. Hunag, "Mechanical Performance and Microstructural Evolution of Rotary Friction Welding of Acrylonitrile Butadiene Styrene and Polycarbonate Rods," *Materials (Basel).*, vol. 16, no. 9, p. 3295, Apr. 2023, doi: 10.3390/ma16093295.

[23] J. Pratama *et al.*, "Tensile and flexural properties of PLA/Fe3O4 composite prepared with a novel powder delivery method and fused filament fabrication," *Prog. Addit. Manuf.*, vol. 9, no. 6, pp. 2143–2174, Dec. 2024, doi: 10.1007/s40964-024-00571-7.

[24] C. Kuo, J. Xu, and C. Lee, "Weld Strength of Friction Welding of Dissimilar Polymer Rods Fabricated by Fused Deposition Modeling," *Polymers (Basel).*, vol. 14, no. 13, p. 2582, Jun. 2022, doi: 10.3390/polym14132582.

[25] S. Anwar, A. U. Rehman, Y. Usmani, and A. M. Al-Samhan, "Influence of Post Weld Heat Treatment on the Grain Size, and Mechanical Properties of the Alloy-800H Rotary Friction Weld Joints," *Materials (Basel).*, vol. 14, no. 16, p. 4366, Aug. 2021, doi: 10.3390/ma14164366.

[26] R. Winiczenko, A. Skibicki, and P. Skoczylas, "The Experimental and FEM Studies of Friction Welding Process of Tungsten Heavy Alloy with Aluminium Alloy," *Appl. Sci.*, vol. 14, no. 5, p. 2038, Feb. 2024, doi: 10.3390/app14052038.

[27] M. J. Troughton, Ed., "Flash-Free Welding," in *Handbook of Plastics Joining*, Second Edi., Boston: Elsevier, 2009, pp. 127–130. doi: 10.1016/B978-0-8155-1581-4.50015-9.

[28] B. Arifvianto, Y. B. Wirawan, U. A. Salim, S. Suyitno, and M. Mahardika, "Effects of extruder temperatures and raster orientations on mechanical properties of the FFF-processed polylactic-acid (PLA) material," *Rapid Prototyp. J.*, vol. 10, no. June, pp. 1761–1775, 2021, doi: 10.1108/RPJ-10-2019-0270.